

**EFFECTS OF THROMBIN ON THE GROWTH OF PANCREATIC
CANCER CELLS AND CANCER ASSOCIATED FIBROBLASTS USING A
MICROFLUIDIC MODEL**

by

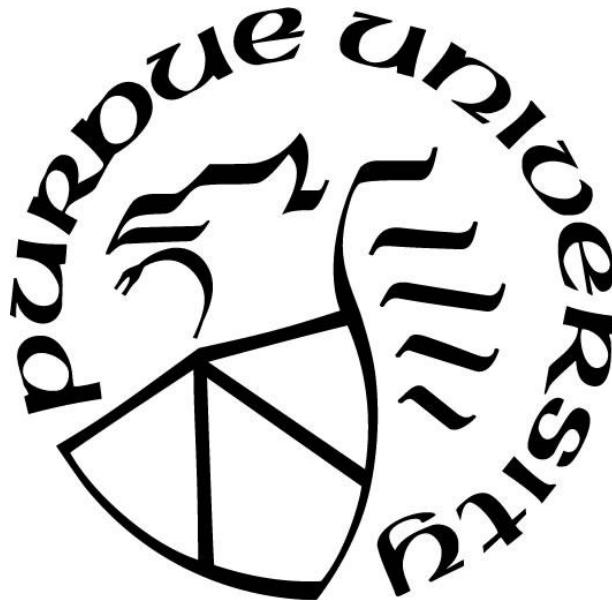
Jonathan Gilvey

A Thesis

Submitted to the Faculty of Purdue University

In Partial Fulfillment of the Requirements for the degree of

Master of Science in Mechanical Engineering



School of Mechanical Engineering

West Lafayette, Indiana

May 2021

THE PURDUE UNIVERSITY GRADUATE SCHOOL
STATEMENT OF COMMITTEE APPROVAL

Dr. Bumsoo Han, Chair

School of Mechanical Engineering

Dr. Andrew Mugler

School of Physics and Astronomy

Dr. Jong Hyun Choi

School of Mechanical Engineering

Approved by:

Dr. Nicole Key

This work is dedicated to my family.

ACKNOWLEDGMENTS

I would like to thank my advisor, Dr. Bumsoo Han, for his guidance, support, and critical questions during the past couple of years. I would like to acknowledge Dr. Jong Hyun Choi and Dr. Andrew Mugler for serving on my committee and their feedback. I am also thankful for the input from my lab mates, specifically Dr. Hye-ran Moon and Dr. Yingnan Shen for their assistance and advice during the course of my research.

TABLE OF CONTENTS

LIST OF TABLES	6
LIST OF FIGURES	7
ABSTRACT	8
1. INTRODUCTION	9
2. METHODS	14
2.1 Reagents	14
2.2 Device Fabrication	14
2.3 Acquisition Of Cell Lines	15
2.4 Cell Culture And Loading Procedure	16
2.4.1 Mouse Cell Lines	16
2.4.2 Human Cell Lines	16
2.5 Chip Loading And Treatment Procedure	17
2.6 Quantification Of Proliferation	17
2.6.1 Mouse Cell Lines	17
2.6.2 Human Cell Lines	18
2.7 Statistical Analysis	19
3. RESULTS	20
3.1 Mouse Cell Lines (Kpc2 And Ostcaf)	20
3.1.1 Kpc2 Proliferation	20
3.1.2 Ostcaf Proliferation	22
3.2 Human Cell Lines (Panc 10.05 And Caf19)	24
3.2.1 Panc 10.05 Proliferation	24
3.2.2 Caf19 Proliferation	26
3.3 Table Of End Of Experiment Results	27
4. DISCUSSION	28
5. CONCLUSION	32
REFERENCES	33
APPENDIX	36

LIST OF TABLES

Table 1: Tabulated results of all studies. Mean values for the increase in the cell area are given and \pm indicates standard deviation.....	27
--	----

LIST OF FIGURES

Figure 1: Microfluidic device “chip” used for 3D culture of cells. The blue regions indicate collagen and cells with the culture area for study in the center of the chip. The red regions are for media. (Media reservoirs are not shown.).....	15
Figure 2: Brightfield images of KPC2 cells.....	20
Figure 3: Fluorescent images of KPC2 cell nuclei, day 0 image is used for normalization.	21
Figure 4: Results from KPC2 proliferation assay. Data points are the mean of the normalized increase in nuclei area and error bars are the standard deviation. No statistically significant difference was observed between the two data sets (for each data point n=3).	21
Figure 5: Brightfield images of OstCAF cells.	22
Figure 6: Fluorescent images of KPC2 cell nuclei, day 0 image is used for normalization.	23
Figure 7: Results from OstCAF proliferation assay. Data points are the mean of the normalized increase in nuclei area and error bars are the standard deviation. No statistically significant difference was observed between the two data sets (for each data point n=3).	23
Figure 8: Fluorescent images of Panc 10.05 cells.....	24
Figure 9: Results from Panc 10.05 proliferation assay. Data points are the mean of the normalized increase in cell membrane area and error bars are the standard deviation. No statistically significant difference was observed between the two data sets (–Thrombin: n=10, +Thrombin: n=8)	25
Figure 10: Fluorescent images of CAF19 cells.....	26
Figure 11: Results from CAF19 proliferation assay. Data points are the mean of the normalized increase in cell membrane area and error bars are the standard deviation. No statistically significant difference was observed between the two data sets (–Thrombin: n=10, +Thrombin: n=7)	27
Figure A-1: Results from KPC2 proliferation assay. Note: The boxed horizontal bar indicates the mean, while the error bars are the standard deviation for that dataset.....	36
Figure A-2: Results from OstCAF proliferation assay. Note: The boxed horizontal bar indicates the mean, while the error bars are the standard deviation for that dataset.	36
Figure A-3: Results from Panc 10.05 proliferation assay. Note: The boxed horizontal bar indicates the mean, while the error bars are the standard deviation for that dataset.....	37
Figure A-4: Results from CAF19 proliferation assay. Note: The boxed horizontal bar indicates the mean, while the error bars are the standard deviation for that dataset.....	37
Figure A-5: ROI for quantifying cell proliferation.	38

ABSTRACT

Thrombotic events are known to be associated with various cancers and recent research has implicated parts of the coagulation system in promoting cancer progression. In particular, thrombin has been studied for its mitogenic effects in 2D cultures as well as in cancer progression in vivo in animal models however, conflicting results exist. Studies of proliferation in response to thrombin stimulation, of pancreatic cancer cells or pancreatic cancer-associated fibroblasts (CAFs) in vitro, that utilize a 3D culture platform are significantly limited. In this study, PDAC cancer cells and cancer-associated fibroblast (CAF) cells were exposed to thrombin using a microfluidic device that mimics in vivo conditions. The cells used herein were cultured in a microfluid device, suspended inside of a 3D collagen matrix, and exposed to daily stimulation of 1 U/mL of thrombin in serum-free media for one hour. The findings of this study are that there is no statistically significant effect, promotive or inhibitory, on the proliferation of the cells used in this study, these results were unexpected. At the end of this paper, a review of potential reasons as to why no significant effect was seen on the cells is presented.

1. INTRODUCTION

The prognosis of pancreatic cancer has a poor outlook with around 24% of those diagnosed surviving past one year and 9% surviving past five years. One of the main reasons for this poor outlook is that the disease is typically not diagnosed until the cancer has already advanced into later stages [1]. Worldwide pancreatic cancer is the seventh leading cause of cancer deaths [2] and in the USA it is the fifth leading cause [3]. In the United State during the year 2021, it is estimated that around 60,430 people will be diagnosed with pancreatic cancer and 48,220 people will perish from pancreatic cancer [4]. Some progress has been made on improving the survival of patients, however, between 2014 and 2017 the 5-year survival rate only increased from 6% to 9% [5]. In 95% of pancreatic cancer cases, the exocrine system is implicated, and these cases have been classified as pancreatic ductal adenocarcinoma (PDAC) [6]. More research and an understanding of the disease's progression are needed to improve the current poor prognosis and marginal improvements in the 5-year survival rate.

Cancers have been recognized to be linked to the coagulation system since at least 1865 when Armand Trousseau published a paper on the subject, ultimately diagnosing himself of the disease and falling ill to gastric cancer [7]. Specifically, Trousseau suggested that thrombosis can be used as a marker for various cancers. Perhaps the most prevalent form of thrombosis which is associated with cancer is venous thromboembolism (VTE). VTE is associated with an increased risk for mortality in cancer patients with the occurrence of fatal pulmonary embolism (PE) being three times more likely in cancer patients [8]. Additionally, cancer patients who are diagnosed with VTE have a worse prognosis, higher rates of mortality, and more aggressive tumors [9]. It has been found that the primary site where cancer develops has been correlated with the frequency of VTE. Notably, cancers of the pancreas, kidney, stomach, lung, uterus, and primary brain tumors lead to a higher incidence of VTE [10]. In patients with pancreatic cancer, there is a significantly increased risk of thrombotic events indicating an activation of the coagulation system and a hypercoagulable state of the patient [11].

The coagulation system is a highly regulated and complex system that regulates the coagulation process so that the wound healing process stays localized and thrombotic events do not occur distant from the site of injury. One of the pathways for coagulation to occur is through tissue factor (TF), which is a transmembrane protein that is one of the key initiators of coagulation

[12]. TF can play role in certain signaling pathways that lead to enhanced tumor growth. Furthermore, many adenocarcinomas over-express TF, and in breast, colorectal, pancreatic, and prostate cancers high levels of TF expression are correlated with poor prognosis, as reviewed by Hisada and Mackman [13].

TF is not the only actor in the coagulation system's promotion of tumor growth. One downstream effect of the coagulation system is the activation of thrombin from the proteolytic cleavage of the zymogen prothrombin. This activated thrombin is then able to cleave soluble fibrinogen to form insoluble fibrin monomers which aggregate to form a blood clot [14]. Additionally, thrombin can activate other downstream targets in the coagulation cascade such as activated protein C, osteopontin, and others not listed here [15],[16]. Thrombin is also able to activate cellular signaling pathways in addition to playing a key role in hemostasis. Some of such pathways come about from protease-activated receptors (PARs). To date, four PARs have been identified in mammals, those being PAR-1, PAR-2, PAR-3, and PAR-4. Thrombin can activate PAR1, PAR-3, and PAR-4 with PAR-1 and PAR-3 having high affinities for thrombin [17]. In human PDAC cells and mouse models, PAR-1 has been identified as being highly expressed when compared to normal pancreatic cells. Also, separately reducing the levels of TF, prothrombin, or PAR-1 expression led to reduced tumor growth in vivo when compared to controls [6]. Additionally, thrombin has been shown to upregulate invasive genes, certain chemokines, angiogenic factors, matrix metalloproteases (MMPs), increase adhesion to the extracellular matrix (ECM) and cellular components, increase chemokinesis, promote drug resistance, and potentially promote dormant tumor cell survival. Further, fibrin formed from thrombin's cleavage of fibrinogen can interact with various integrins and receptors, leading to altered cellular behaviors and promotion of angiogenesis, as reviewed by Wojtukiewicz et al. [18].

Following the discussion above a key question arises. Are TF, thrombin, and PAR-1 an axis for promoting tumor progression? With TF activating thrombin which then activates PAR-1. This study focuses on thrombin's mitogenic effect on PDAC cell lines and pancreatic cancer-associated fibroblasts. As a result, what follows is a review of the current studies on thrombin's effects on these and related cells.

Thrombin's effect on cancer cells has been studied in vitro by various researchers, although data for pancreatic cancer cells is lacking. Zain et al. used a 2D culture to investigate thrombin concentration-dependent effects on cancer cells of various types. They found that the degree of

cell proliferation was dependent on the concentration of thrombin present in the media [19]. Darmoul et al. exposed HT-29 colorectal cancer cells to approximately 1 U/mL of thrombin in 2D culture using serum-free media and observed around a 400% increase in cell proliferation [20]. Interestingly there are conflicting results between Zain and Darmoul when comparing the two colorectal cell lines used and this may be linked to the different treatment protocols.

In vivo studies have indicated that the coagulation system plays a role in tumor progression. Yang et al. used KPC cells and a mouse model and discovered that lowering prothrombin levels in the mice (~10% of normal) led to tumors with significantly diminished growth. In addition, reducing PAR-1 expression of the tumor cells led to reduced or no tumor growth, while reducing PAR-1 in the tumor microenvironment had little impact on reducing tumor growth [21]. Tekin et al. utilized an orthotopic pancreatic cancer model and found that PAR-1 expression was correlated with cellular mesenchymal characteristics and reduced tumor growth, with the loss of PAR-1 increasing tumor cell differentiation and increased tumor growth [22], conflicting with the results by Yang et al.. Further, Queiroz et al. reduced the PAR-1 expression in the TME and found that reducing PAR-1 expression led to a decreased tumor size [23]. Perhaps inconsistency between these results and those by Yang et al. is due to the different cell lines being used. Adams et al. analyzed colon and melanoma cancer cell tumor growth in mice with reduced (~10% of normal) prothrombin levels and found that tumors composed of the colon cancer cells had a significant reduction in their growth while melanoma cancer cells remained unaffected, indicating a cancer cell origin dependent effect of thrombin. Additionally, the researchers found that tumor growth was hindered with either reduction of PAR1 expression or a reduction of fibrinogen [24].

The interaction of pancreatic cancer cells with the stroma has been recognized as an important aspect of PDAC progression [25],[26],[27]. PDAC is characterized by a desmoplastic environment surrounding the tissue, and the stroma in pancreatic cancer can form up to 90 % of the tumor microenvironment [26]. The stroma surrounding the tumor is complex and consists of the ECM, various signaling molecules, extracellular vesicles, and a variety of different cell types present within the tissue. Additionally, the stiffness of the ECM itself has been shown to alter tumor cell behavior, such as promoting dormant tumors [28], promoting epithelial to mesenchymal transition, and giving rise to drug resistance against certain commonly used chemotherapeutic drugs [25]. The stromal tissue primarily consists of fibroblasts that secrete and remodel the ECM, as well as secreting other factors influencing various types of cells. Further, the fibroblasts

themselves respond to the local environmental cues such as ECM composition and other chemical signals, and in certain cases, this can lead to excessive fibrosis [29]. Resident fibroblasts, or fibroblasts from other sources, within the pancreatic tissue can be reprogrammed to become cancer-associated fibroblasts (CAFs). These CAFs are fibroblasts that differ from quiescent fibroblasts and are found in the tumor microenvironment (TME). In PDAC, CAFs lead to a fibrotic environment as well as secreting other factors which lead to increased tumor progression [30].

Fibroblast proliferation in response to thrombin has been quantified by others, although data for CAFs is lacking. Hall and Ganguly utilized a 2D culture and found that the degree to which human fibroblast's growth was stimulated depended on the thrombin concentration as well as the time between stimulating the cells and subculturing [31]. Snead and Insel used a 2D culture and found evidence that activation of PAR-1 via thrombin, on cardiac fibroblasts, leads to increased collagen deposition and a myofibroblast morphology without a significant increase in fibroblast proliferation [32]. Pohl, Bruhn, and Christophers used a 2D culture with skin fibroblast and observed that fibroblast proliferation increased with thrombin exposure following a dose-dependent trend [33]. D'Andrea et al. observed that PAR-1 expression was up-regulated in proliferating, alpha-SMA positive, fibroblasts that surrounded malignant carcinoma cells [34]. The results presented above provide evidence that thrombin exposure may significantly increase the proliferation or activity of fibroblasts and CAFs and potentially lead to increased desmoplasia.

To date, most all in vitro studies involving thrombin's proliferative effects have relied on 2D culture methods to study the effect of thrombin on cancer cells. While these 2D cell cultures are cheap and owe themselves to high throughput, they fail to capture various components of the in vivo tumor microenvironment such as cell-matrix interactions as well as cell-cell interactions in 3D. It should be noted that cell responses to treatment can differ drastically between 2D and 3D cultures. While animal models are useful they are expensive, time-consuming, and do not always accurately model the human TME. The use of 3D cell cultures allows one to model treatments on human cell lines in an environment that more closely resembles in vivo conditions [26]. In this study a tumor-microenvironment-on-chip (T-MOC) microfluidic device is used for 3D culture of cells, the same chip geometry has also been employed successfully for various experiments by others [35]–[37]. Using a microfluidic device to study the effects of various biomolecules on cells is superior to 2D studies due to realistic cell-matrix and cell-cell interactions, the formation of niche regions and 3D structures, spatially varying nutrient concentrations, accurate cell

morphology, phenotype, polarity, and division characteristics [38]. Additionally, the use of a 3D culture in a microfluidic device is unique due to tight control over the cell culture conditions, the use of species-specific cells, live imaging of cells in culture conditions, low cost, and the potential for high throughput experiments.

The *in vivo* studies demonstrate the importance of the coagulation system, specifically thrombin and/or PAR-1 in the context of tumor growth. However, these animal models are highly complex, time-consuming, and expensive to work with. They also have many other cellular components, making it hard to determine the exact role that thrombin or PAR-1 plays in tumor progression. The *in vitro* studies that have been employed previously use extended serum starvation which makes it difficult to determine if thrombin would lead to a mitogenic effect under normal growth conditions. Additionally, previous *in vitro* studies have primarily used 2D cultures which lack a realistic 3D environment that the cells natively reside in. Furthermore, most of the data for fibroblasts that has been reviewed applies to thrombin's effects on normal fibroblasts and not CAFs. Thus, this study will investigate whether or not intermittent thrombin stimulation leads to an increase or decrease in the proliferation of PDAC cancer cells and CAFs.

2. METHODS

2.1 Reagents

Mouse cell lines were cultured in cytiva (formerly GE Healthcare Life Sciences) HyClone RPMI 1640 supplemented with L-glutamine (cytiva, Marlborough, MA) the media was supplemented with 5% fetal bovine serum (FBS) (Fisher Scientific, Waltham, MA) and 1% penicillin/streptomycin (P/S) (10,000 U/mL) (Fisher Scientific, Waltham, MA). Advanced DMEM/F-12 (Gibco, Carlsbad, CA) was supplemented with 10% FBS, 1% L-glutamine (200 mM) (Gibco, Carlsbad, CA), and 1% P/S. 1X DPBS with calcium and magnesium (Gibco, Carlsbad, CA) and Trypsin-EDTA (0.05%) (Gibco, Carlsbad, CA) was used to wash and harvest cells. Collagen gels were produced using Corning collagen 1, high concentration, rat tail (Corning, Corning, NY), this was mixed with 10X PBS (Gibco, Carlsbad, CA), 1 M sodium hydroxide solution (Sigma-Aldrich, St. Louis, MO), HEPES (1 M) (Gibco, Carlsbad, CA), P/S, L-glutamine, FBS, and DI water. Bovine α -thrombin stock solution at 1000 U/mL (Enzyme Research, South Bend, IN) was used for stimulating the cells with thrombin, this was diluted to 1 U/mL in serum-free media for treating cells. Hoechst 33342 (Sigma Aldrich, St. Louis, MO) was used to stain the mouse cell nuclei for quantification of proliferation. Before use in experiments, all cells were cultured in Falcon tissue culture treated flasks (Fisher Scientific, Waltham, MA). Polydimethylsiloxane (PDMS) (Midland, MI) was used to create the microfluidic devices.

2.2 Device Fabrication

The devices used in this study were fabricated out of PDMS using a soft lithographic process. The base liquid was mixed thoroughly with the curing agent at a 10:1 ratio. The mixture was then poured over molds and degassed in a vacuum chamber. After degassing any remaining bubbles were removed by gently using a stream of air to pop any remaining air bubbles. The molds were then placed on a hot plate at 80 °C for eight hours. After curing the PDMS was removed from the molds and then 2 mm diameter holes were made in the PDMS for collagen loading as well as media channels. The surface of the chip was then cleaned four times by the use of scotch magic tape. The PDMS chip and a glass microscope slide were treated with a handheld corona discharger (Electro-Technic Products, Chicago, IL), and then the two treated surfaces were mated together.

The assembly was placed on a hot plate at 120 °C for eight hours. A rendering of the chip on a glass slide can be seen in Figure 1.

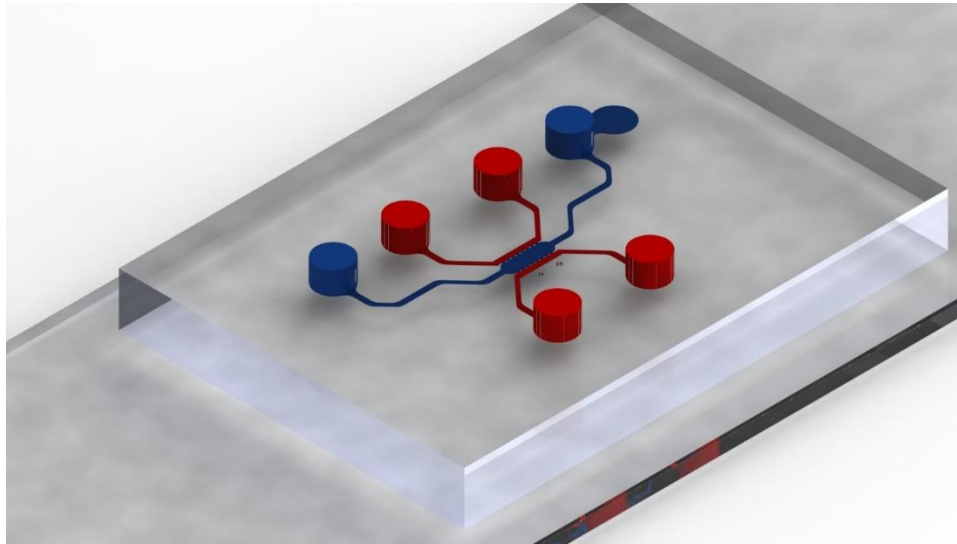


Figure 1: Microfluidic device “chip” used for 3D culture of cells. The blue regions indicate collagen and cells with the culture area for study in the center of the chip. The red regions are for media. (Media reservoirs are not shown.)

2.3 Acquisition of Cell Lines

The cell line KPC2 was acquired from Dr. Konieczny’s lab (Purdue University) and is a murine pancreatic cancer cell. The cell line OstCAF is of murine origin and was provided from Dr. Fishel’s lab (Indiana University). Both mouse cell lines were cultured in RPMI 1640 with 5% FBS and 1% P/S as described below.

The cell line Panc 10.05 and CAF19 cell lines were acquired from the Fishel Lab (Indiana University). Panc 10.05 is a human pancreatic cancer cell line and CAF19 cells are human cancer-associated fibroblasts of pancreatic origin. Both human cell lines were cultured in DMEM with 10% FBS, 1 % L-glutamine, and 1% P/S as described below.

2.4 Cell Culture and Loading Procedure

2.4.1 Mouse cell lines

KPC2 and OstCAF cell lines were cultured in serum containing RPMI 1640 and incubated at 37 °C and 5% CO₂ under normal culture conditions. The KPC2 cells were sub-cultured every three days splitting the cells at approximately a 1:10 ratio. Subculture was performed by washing the cells twice with 1X PBS and then adding trypsin and placing the flask in an incubator at 37 °C and 5% CO₂ for six minutes. The cells were then separated via centrifugation at 1200 RPM for five minutes in a centrifuge using a TX-400 rotor (Fisher Scientific, Waltham, MA). OstCAF cells were split every five days at a 1:3 ratio. Subculture was performed by washing the cells twice with 1X PBS and then adding trypsin and placing the flask in an incubator at 37 °C and 5% CO₂ for three minutes. The cells were then separated via centrifugation at 1200 RPM for five minutes.

For all mouse cell lines, the media was exchanged every day until the cells were ready to be harvested. No cells were used in experiments beyond passage 10.

2.4.2 Human cell lines

Panc 10.05 and CAF19 cells were cultured in serum containing DMEM 1640 and incubated at 37 °C and 5% CO₂ under normal culture conditions. Panc 10.05 and CAF19 were sub-cultured every five days splitting the cells at approximately a 1:10 ratio. Panc 10.05 subculture was performed by washing the cells twice with 1X PBS and then adding trypsin and placing the flask in an incubator at 37 °C and 5% CO₂ for eight minutes. The cells were then separated via centrifugation at 125 G for five minutes. CAF19 subculture was performed by washing the cells twice with 1X PBS and then adding trypsin and placing the flask in an incubator at 37 °C and 5% CO₂ for four minutes. The cells were then separated via centrifugation at 125 G for three minutes.

For all human cell lines, the media was exchanged every day, except for the day directly after passaging, until the cells were ready to be harvested. No cells were used in experiments beyond passage 10.

2.5 Chip Loading and Treatment Procedure

Before loading the chips, the specific cell type was harvested as described above. They were then suspended in chilled 6 mg/mL type-1 collagen solution on ice at a concentration of 10^6 cells/mL. The solution was kept on ice during the loading process, and the loading of all chips was complete within 30 minutes. After a chip was loaded it was placed into an incubator at 37 °C and 5% CO₂ for 75 minutes for the collagen to polymerize.

The thrombin treatment procedure for all cell lines was the same. After 75 minutes in the incubator, the chips were moved to a biosafety hood where reservoirs for media were added. Then 200 µL of serum-free media containing either 0 or 1 U/mL of was added to one reservoir on each side of the chip so that media would flow through the channels and thrombin would be free to diffuse into the collagen/cell region. After the media was added the chips were placed into the incubator for 30 minutes. Following this, the media was aspirated and fresh serum-containing media was added to the reservoirs. 600 µL total was added to one side of the chip and 400 µL total was added to the other side. The chips were then imaged using a fluorescent microscope. After imaging, the chips were placed back into the incubator. On the next day, the media was aspirated and 400 µL of serum-free media was added to one side of the chips, the chips were then placed in the incubator for two hours. After the two hours, the media was aspirated and 400 µL of serum-free media containing either 0 or 1 U/mL thrombin was added to the same side of the chips as in the previous step, the chips were then placed in the incubator for one hour. Following this, the media was aspirated and then serum-containing media was added. 600 µL total was added to one side of the chip and 400 µL total was added to the other side as on day 0. This process was repeated until the end of the experiment. No treatment or media exchange was performed on the last day of the experiment.

The solution with serum-free media and thrombin was discarded after five days as activated thrombin is not stable. When not in use the solution was kept in a refrigerator at 4 °C.

2.6 Quantification of Proliferation

2.6.1 Mouse cell lines

Quantification of KPC2 and OstCAF cell lines was performed by nuclear staining. For KPC2, quantification was performed on days 0, 2, and 3 while for OstCAF quantification was

performed on days 0, 1, and 3. On the day of quantification, two chips were selected randomly from each treatment group. The media was aspirated and 400 μL of media containing Hoechst 33342 was added to a reservoir on one side of the chips. The chips were then placed in the incubator for 30 minutes. After incubation, the media was aspirated and then the chips were washed with PBS for approximately 30 minutes. Fluorescent images were then taken of the chips with a 10X objective. Seven focal planes were used in the imaging each spaced 20 μm apart. Images were taken on either side of the cell culture area due to the cell culture area being wider than the microscope's field of view. The region of interest relative to the chip geometry is shown in the appendix in Figure 16. The stained chips were discarded on the day of staining as the staining process can potentially interfere with experimental results. ImageJ was used to quantify the nuclei area. First, the 10X images were lined up, cropped and then a gaussian-based stack focuser was applied with a radius of 5 pixels. WEKA Segmentation was used on the images to segment the nuclei areas. One of the data sets on day 0 was selected randomly to normalize the relative increase in nuclei area for that experimental run. The normalized nuclei area for each experiment was calculated by dividing the nuclei area on each day by the nuclei area on day 0. Each experiment was repeated three times.

2.6.2 Human cell lines

Quantification of Panc 10.05 and CAF19 cell lines was performed by imaging the cell membranes. This was possible as the Panc 10.05 cell line is transfected with TdTomato while CAF19 is transfected with GFP. For Panc 10.05 and CAF19 the cells were imaged daily, and no chips were discarded as staining was not necessary to image the cells. A 4X objective was used and seven focal planes were used in the imaging each spaced 20 μm apart. The region of interest relative to the chip geometry is shown in the appendix in Figure 16. ImageJ was used to process the images. The images were cropped, and then the gaussian-based stack focuser was applied with a radius of 2 pixels. WEKA Segmentation was used on the images to segment the cell membrane areas. The day 0 area was used to normalize the relative increase in cell area for each individual chip. The normalized cell area for each experiment was calculated by dividing the cell area on each day by the cell area on day 0. Each experiment was repeated three times.

2.7 Statistical Analysis

A two-tailed t-test was applied between the control (–thrombin) and test case (+thrombin). A two-tailed test was chosen as it was not known whether the thrombin treatment would lead to increased or decreased cell proliferation. In all cases no statistically significant differences were seen between the control groups ($p > 0.55$ for all cases)

3. RESULTS

3.1 Mouse Cell Lines (KPC2 and OstCAF)

3.1.1 KPC2 Proliferation

Brightfield images from the KPC2 proliferation assay are presented in Figure 2. The cells in Figure 3 are stained with Hoechst 33342. Figure 4 shows the normalized mean increase in nuclei area on each day.

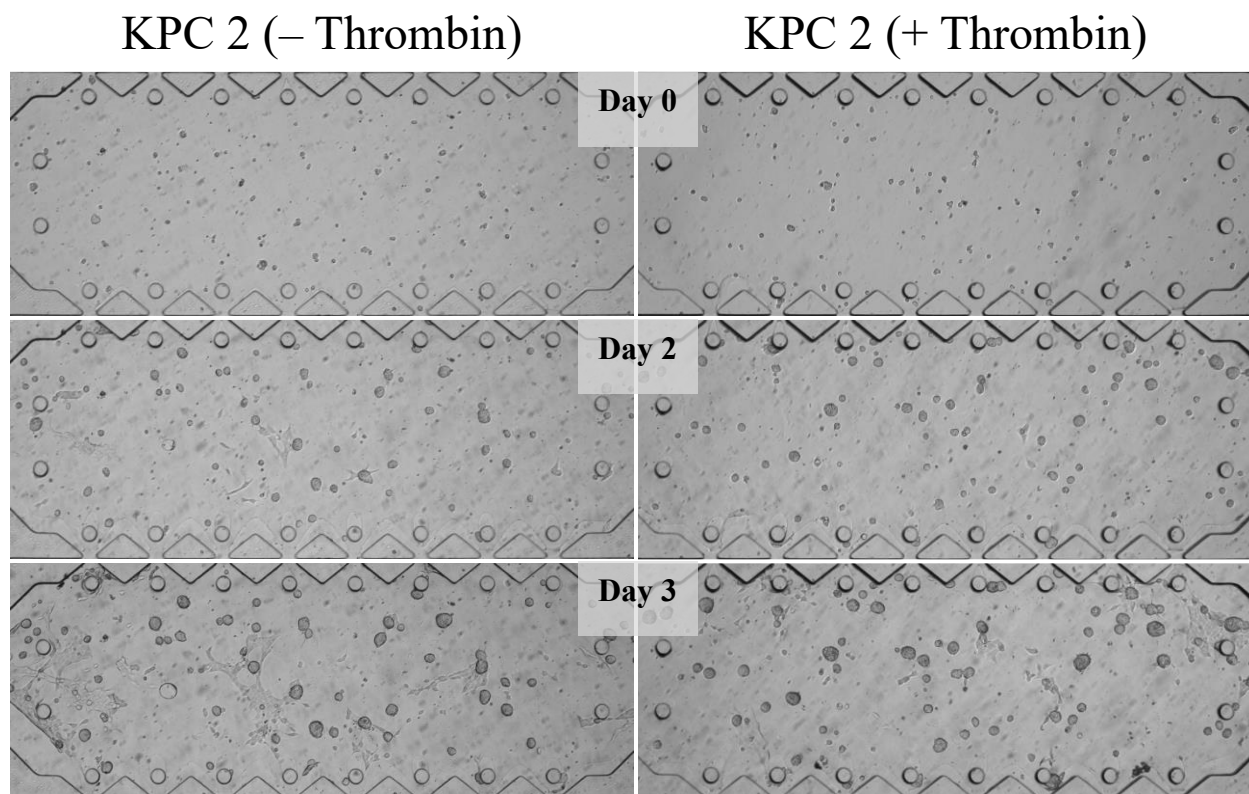


Figure 2: Brightfield images of KPC2 cells.

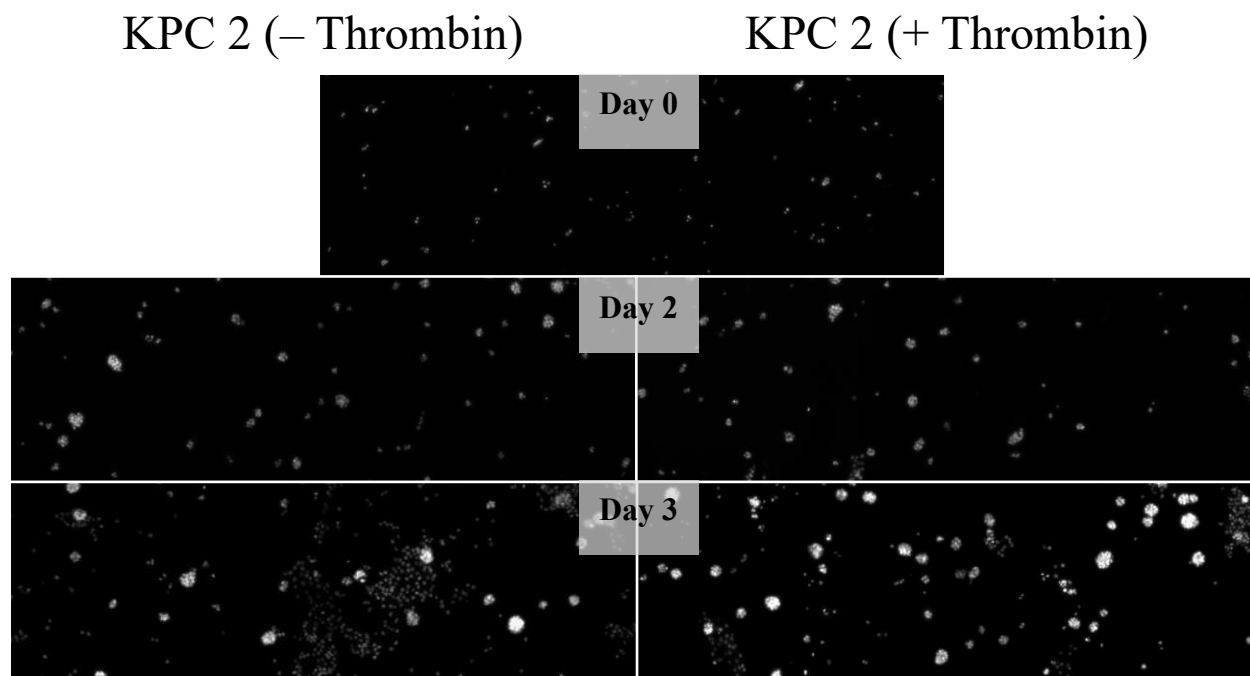


Figure 3: Fluorescent images of KPC2 cell nuclei, day 0 image is used for normalization.

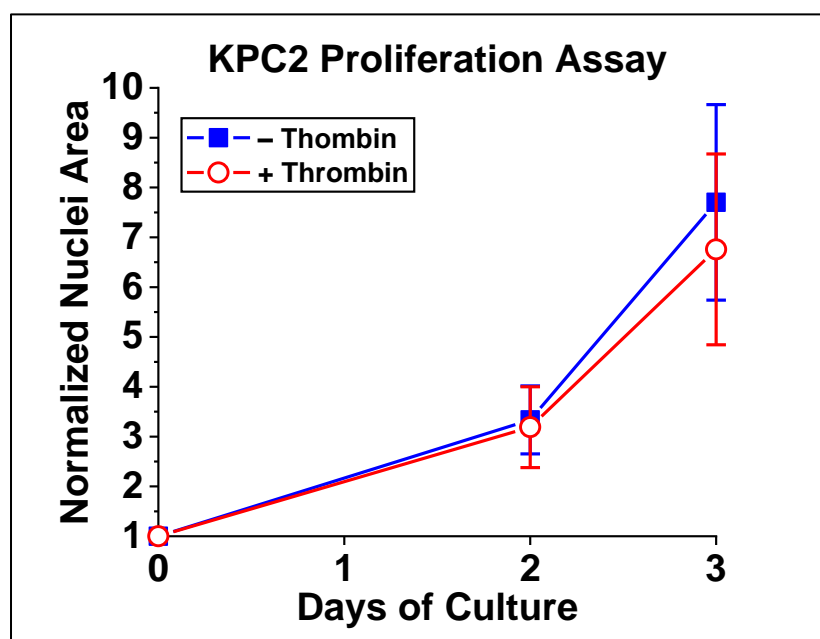


Figure 4: Results from KPC2 proliferation assay. Data points are the mean of the normalized increase in nuclei area and error bars are the standard deviation. No statistically significant difference was observed between the two data sets (for each data point n=3).

3.1.2 OstCAF Proliferation

Brightfield images from the OstCAF proliferation assay are presented in Figure 5. The cells in Figure 6 are stained with Hoechst 33342. Figure 7 shows the normalized mean increase in nuclei area on each day.

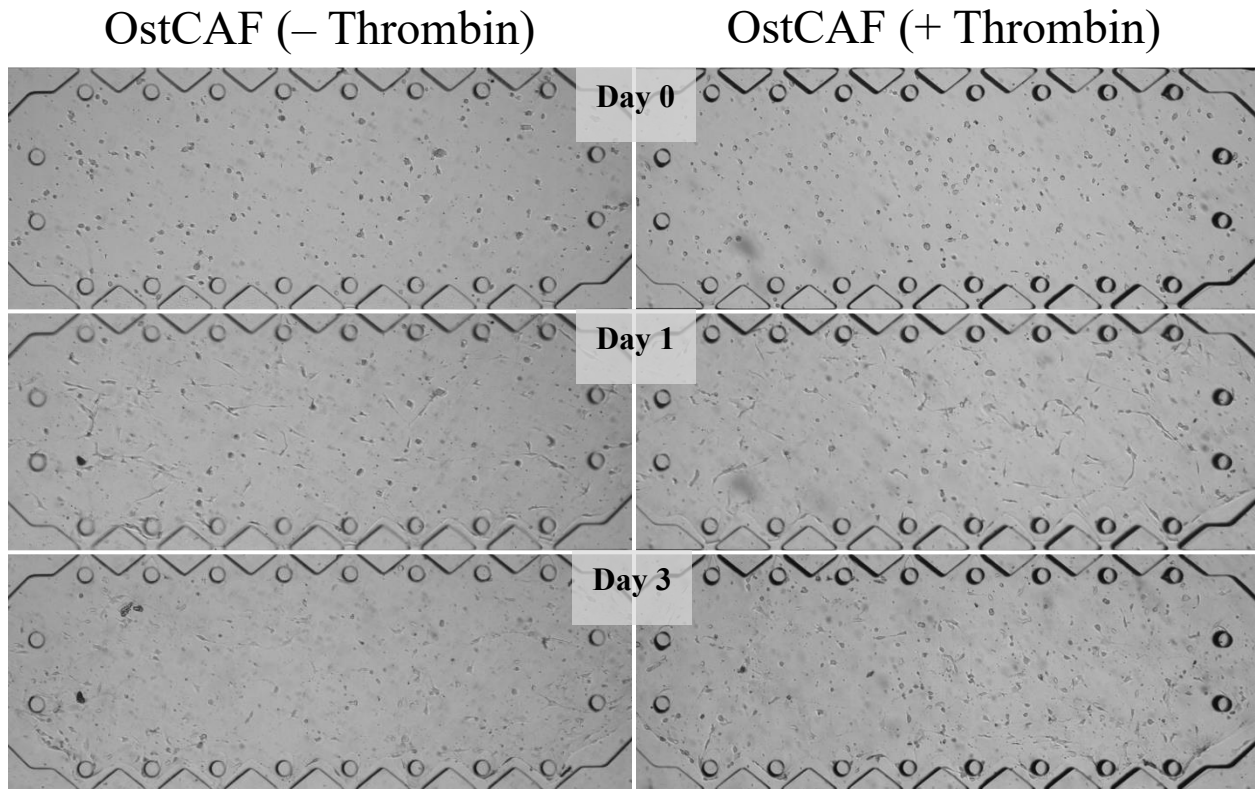


Figure 5: Brightfield images of OstCAF cells.

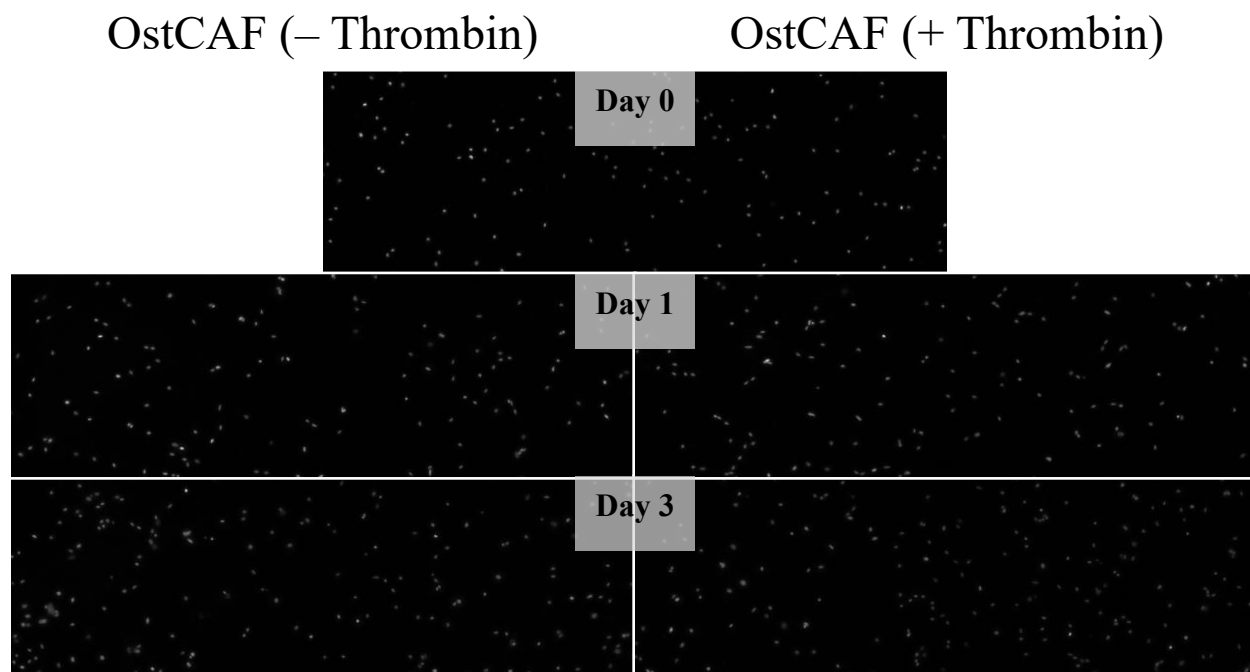


Figure 6: Fluorescent images of KPC2 cell nuclei, day 0 image is used for normalization.

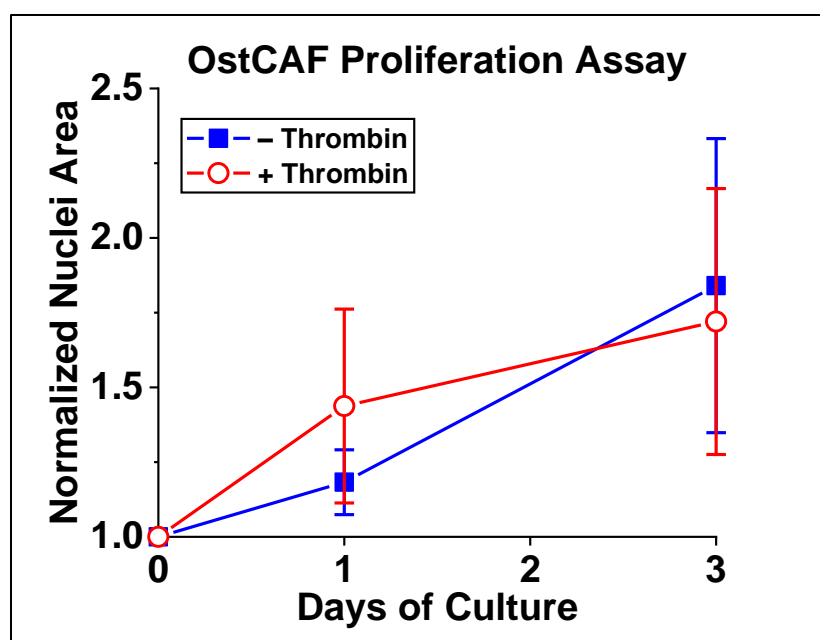


Figure 7: Results from OstCAF proliferation assay. Data points are the mean of the normalized increase in nuclei area and error bars are the standard deviation. No statistically significant difference was observed between the two data sets (for each data point n=3).

3.2 Human Cell Lines (Panc 10.05 and CAF19)

3.2.1 Panc 10.05 Proliferation

Fluorescent images from the Panc 10.05 proliferation assay are presented below in Figure 8. The cells fluoresce as they are transfected with TdTomato as previously mentioned. Figure 9 shows the mean increase in the cell area.

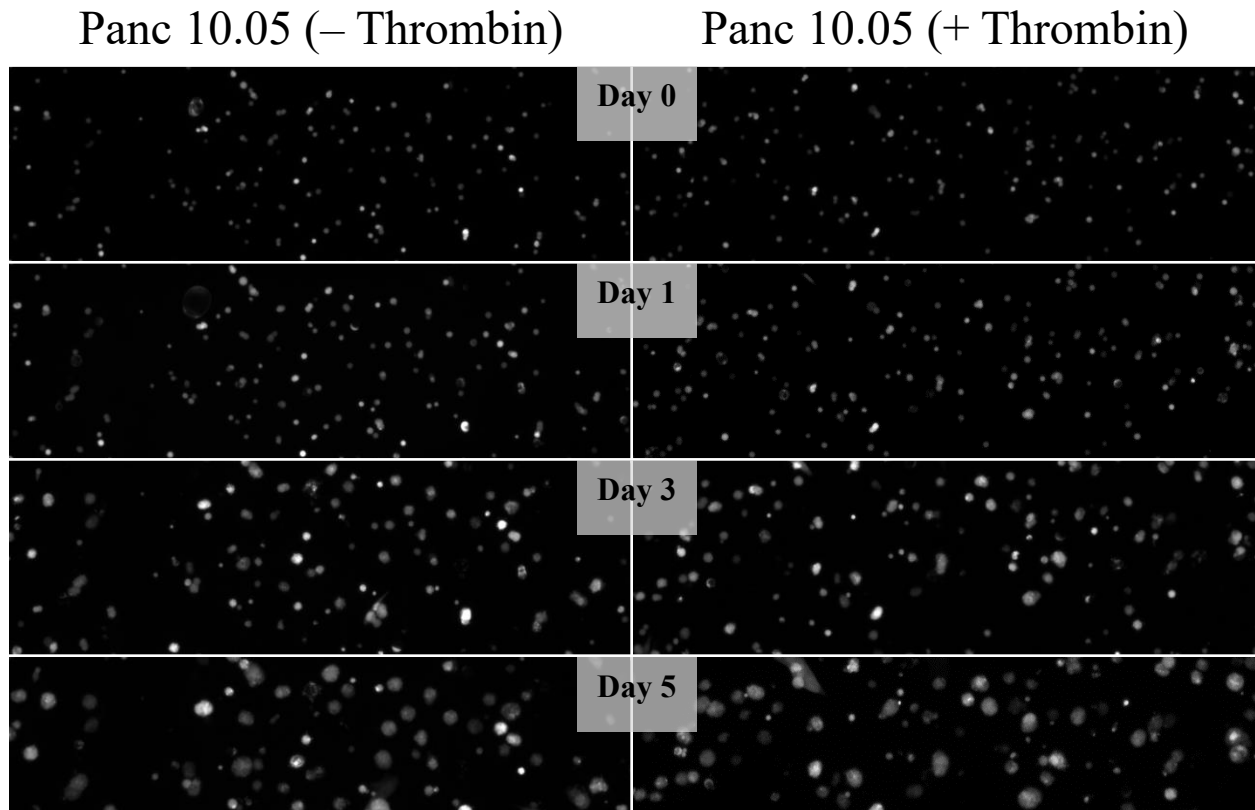


Figure 8: Fluorescent images of Panc 10.05 cells

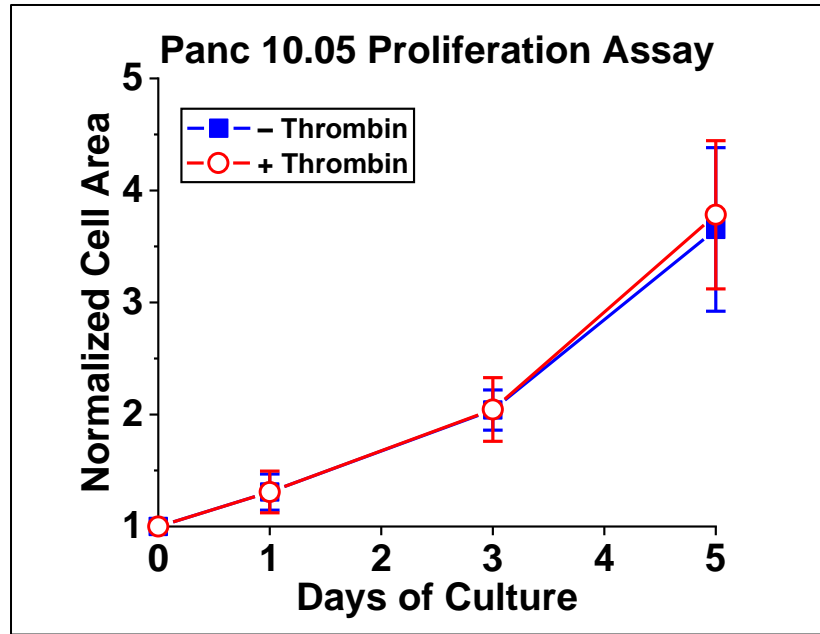


Figure 9: Results from Panc 10.05 proliferation assay. Data points are the mean of the normalized increase in cell membrane area and error bars are the standard deviation. No statistically significant difference was observed between the two data sets (-Thrombin: n=10, +Thrombin: n=8)

3.2.2 CAF19 Proliferation

Fluorescent images from the CAF19 proliferation assay are presented below in Figure 10. The cells fluoresce as they are transfected with GFP as previously mentioned. Figure 11 shows the mean increase in the cell area.

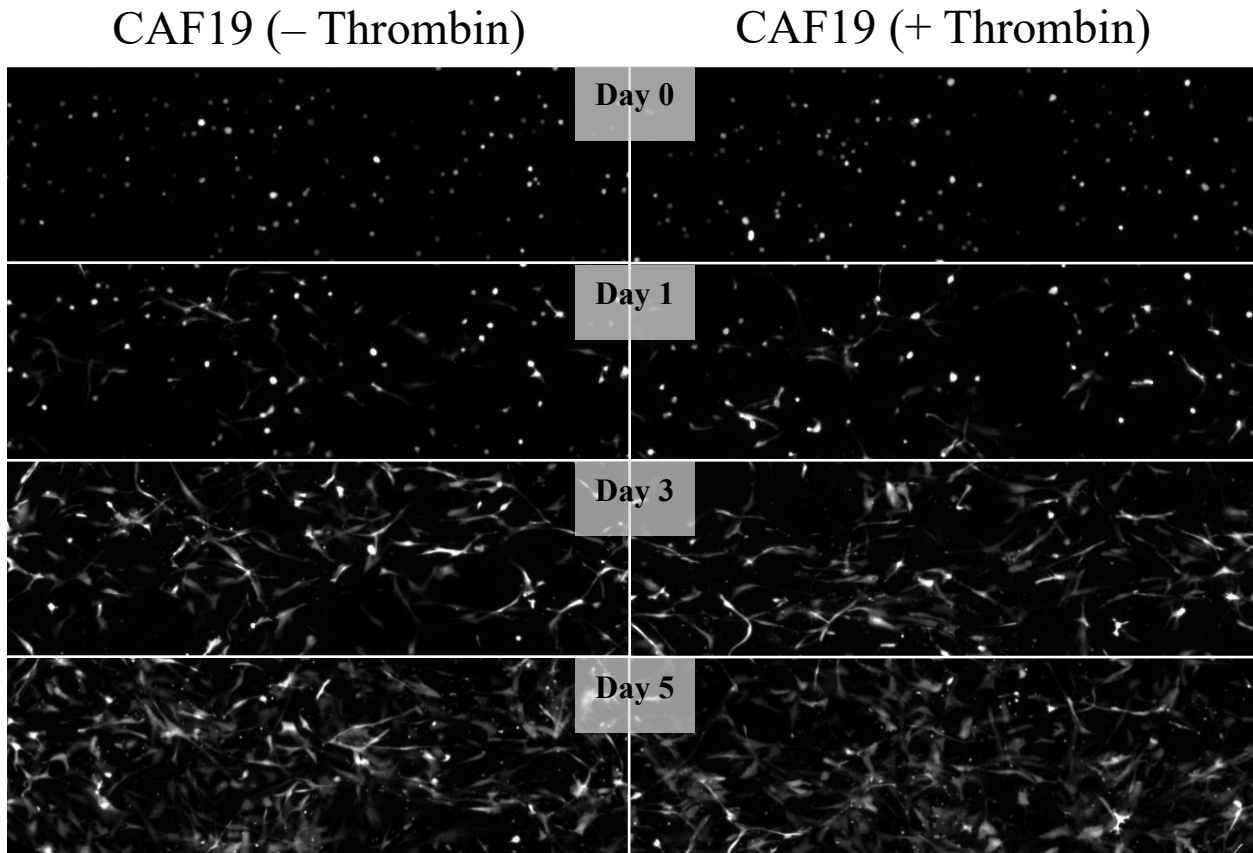


Figure 10: Fluorescent images of CAF19 cells.

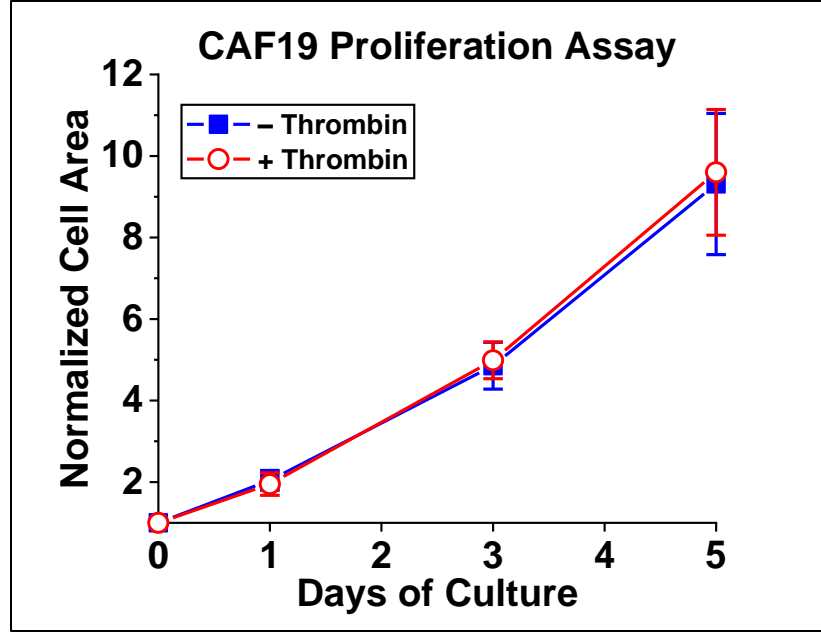


Figure 11: Results from CAF19 proliferation assay. Data points are the mean of the normalized increase in cell membrane area and error bars are the standard deviation. No statistically significant difference was observed between the two data sets (–Thrombin: n=10, +Thrombin: n=7)

3.3 Table of End of Experiment Results

Table 1 lists the results for the mean values of each study where \pm indicates the standard deviation. For further info see figures A-1 through A-4 in the appendix that detail the results of each experimental run.

Table 1: Tabulated results of all studies. Mean values for the increase in the cell area are given and \pm indicates standard deviation.

	Relative Area Increase (mean \pm standard deviation)			
	Day 3 Nuclei Area Increase		Day 5 Cell Area Increase	
	KPC2	OstCAF	Panc 10.05	CAF19
–Thrombin	7.70 \pm 1.96	1.84 \pm 0.49	3.65 \pm 0.73	9.31 \pm 1.73
+Thrombin	6.76 \pm 1.92	1.72 \pm 0.44	3.78 \pm 0.66	9.60 \pm 1.54

4. DISCUSSION

The hypothesis, that intermittent stimulation of pancreatic cancer and CAF cells with thrombin would lead to increased proliferation appears to be incorrect. As tabulated in Table 1, at the end of the three-day experiment the relative increase in nuclei area of KPC2, with the standard deviation, was 7.70 ± 1.96 without thrombin and 6.76 ± 1.92 with thrombin. OstCAF increased by 1.84 ± 0.49 without thrombin and 1.72 ± 0.44 with. For the human cell lines at the end of the five days, the relative increase in the cell area of Panc 10.05 was 3.65 ± 0.73 without thrombin and 3.78 ± 0.66 with. CAF19 increased by 9.31 ± 1.73 without thrombin and 9.60 ± 1.54 with.

The results from the experiments were unexpected. It is difficult to point to a reason as to why no significant increase in cell proliferation was observed, however, some previous studies may shed some light on the results. However, it is strange that in this study no significant effect was seen on the proliferation or hindrance of cell growth as those mentioned in the intro and below have observed. It is suspected that the intermittent thrombin treatment was not sufficient to lead to a significant, proliferative or restrictive, effect on cell proliferation.

One reason that proliferation was not seen in the cells could have been due to the absence of serum during thrombin exposure. Serum was not included as the serum contains various factors which could lead to the deactivation of thrombin such as antithrombin. Others who have observed an increase in proliferation during serum starvation may have been observing thrombin acting as an antiapoptotic factor instead of a mitogen. [39] Including serum with thrombin could have led to different effects as thrombin acts on other biomolecules in the serum such as protein C [15] or osteopontin [16]. While this may be a key mechanism in thrombin's mitogenic effect it is not of interest in this study. Previous researchers investigating thrombin's role on cell proliferation have included serum during their thrombin exposure studies [19], [31] or have used in vivo models [21], [23], [24] Thus, in these studies one cannot be sure that thrombin is the key player promoting cell proliferation or if it is some downstream biomolecule(s) in the serum that is leading to this behavior. For example, Adams et al. found that fibrinogen levels were correlated with colon cancer progression [24]. While Yang et al. identified PAR1 activation by thrombin as playing a role in immune evasion.

The 3D matrix used to suspend the cells in this study could also have been a factor in hindering the proliferation of the cells. It is well known that tissue stiffness and composition play a role in cellular behavior [25]. The 3D collagen matrix may lack some key chemical, mechanical, or transport property that is found in the 2D or in-vivo environments. Without these additional cues, the cells may not be processing the mitogenic signal from the stimulation of thrombin.

Another factor that could have contributed to the lack of mitogenic effect of the thrombin is from the concentration used, or that the treatment was intermittent. Pohl et al. found that stimulating fibroblasts, in their log growth phase, with 1 U/mL thrombin was insufficient to act as a mitogen. Although their study differed from the one here as they used a 2D culture and stimulated the cells for 12 hours in serum-free media [33]. Hall and Ganguly, observed that thrombin hindered fibroblast growth when added shortly after freshly passaging cells in subconfluent cultures, however, thrombin acted as a mitogen if the cells were allowed to become more established. They also found that serum levels in the media play a role in thrombin's proliferative effects [31]. Concentration is also suspected as Zain et al. found that thrombin concentration has a biphasic effect on cancer cell proliferation. At low concentrations around 0.5 U/mL and under thrombin acted as a mitogen while at higher concentrations around 1 U/mL and higher thrombin's effect was that it hindered cell growth. Interestingly, this effect was attenuated when the serum concentration was increased [19]. There is a possibility that the concentration and treatment used were right at the cusp of leading to proliferation or hindrance in cell growth. Another discrepancy in the degree to which the cells are exposed to thrombin could be from a lack of fibrin in this study. Upon clot formation activated thrombin can bind to fibrin this bound thrombin can avoid deactivation and remain in the fibrin clot [40]. This bound-up thrombin could be acting as a reservoir for thrombin leading to extended stimulation of the cells. Additionally, fibrin may alter cellular proliferation and survival through mechanical and chemical cues [28].

In vivo thrombin's effect on the TME could be more complicated than its action as a mitogen. For example, Schweickert et al. have identified certain genes which are linked to immunosuppression that become upregulated following thrombin's activation of PAR1 [41]. Additionally, the present study only included monocultures which is not the case with in vivo studies. It has been found that cancer cells and CAFs signal to each other through chemical

and mechanical cues and that the interaction between the two can lead to enhanced tumor growth and invasiveness. CAFs secrete factors that can lead to epithelial-mesenchymal transition resulting in a mesenchymal phenotype [42]. The effects of thrombin on these mesenchymal phenotype cancer cells are unknown. There may be some interaction between thrombin, cancer cells, and CAFs that leads to increased proliferation or an increase in invasiveness that has not yet been revealed. This study also lacked an immune system component, and PAR-1 signaling in vivo seems to play a role in immune evasion via recruitment of immunosuppressive cells, as researched by Yang Et al. [21]. Furthermore, PAR-1 can be activated by a host of other biomolecules such as MMP-1, MMP2, MMP-9, MMP-13, APC, plasmin, factor Xa, granzyme A, TF-FVIIa [39], and others not listed here. The PAR-1 mediated downstream signaling events depend on the activating factor and can further be modulated by other synergetic or antagonistic pathways.

Fibrin may also be able to act as a cue for cells to proliferate via certain signaling pathways. For example, Pohl et al. observed a fibrin concentration-dependent increase in fibroblast proliferation, although their study lacked other ECM components native to the TME such as collagen.[33] Adams et al. found that fibrinogen deficient mice had reduced tumor size and abnormal vasculature. However, it was not known to the researchers if fibrinogen leads to abnormal vasculature or if it is a byproduct of some other fibrin(ogen) dependent mechanism [24]. Furthermore, the tumorigenic effects of fibrin in vivo could be linked to a role in promoting immune evasion thereby promoting cancer progression [43].

Varying suspicions as to why no deviation in the proliferation of the cultured cells are given above. Comparing with works by other researchers it is suspected that intermittent thrombin stimulation was insufficient to induce an increase or decrease in proliferation. Further, the method of quantifying the cell proliferation relies on measuring the cross-sectional area of cells in a 3D culture. This may underestimate the proliferation of cells as there are differences in the projected areas of the cells depending on their spatial positions. For example, the same number of cells maintaining a clumped, spheroid shape will have a lesser projected area than if those cells were spread about in a 2D morphology. Future studies should focus on improving quantifying cell proliferation in 3D cultures and elucidating the mechanisms through which thrombin promotes pancreatic cancer growth by altering the concentration and exposure time, as well as including other cell types and various other downstream targets of thrombin.

Recovery of the sample would allow for gene expression to be quantified and may elucidate some key differences between cells exposed to thrombin in 2D and 3D cultures.

5. CONCLUSION

This study utilized a 3D cell culture on a microfluidic device to study the effect of thrombin stimulation on cancer cells in a 3D environment. WEKA image segmentation was used to quantify the areas of either the cell nuclei or cell membrane in order to infer the level of proliferation. It was found that stimulating pancreatic cancer cells and CAF cells for one hour daily had a negligible effect on the cancer cells and cancer-associated fibroblasts proliferation. Other studies have suggested that thrombin acts as a mitogen in vitro and in vivo, conflicting with the results from this study. More work is needed to elucidate the mechanism through which the coagulation system promotes cancer progression. Identifying the key mechanisms in this axis may bring about new therapeutic targets and new insight into how the coagulation system interacts with cancer cells. These findings will likely have impacts on other cancers, especially those which are associated with the coagulation system. Also, certain biomarkers may be discovered for persons with pancreatic cancer enabling earlier detection and improved prognosis.

REFERENCES

- [1] P. Rawla, T. Sunkara, and V. Gaduputi, "Epidemiology of Pancreatic Cancer: Global Trends, Etiology and Risk Factors," *Rev. World J Oncol*, vol. 10, no. 1, pp. 10–27, 2019, doi: 10.14740/wjon1166.
- [2] F. Bray, J. Ferlay, I. Soerjomataram, R. L. Siegel, L. A. Torre, and A. Jemal, "Global cancer statistics 2018: GLOBOCAN estimates of incidence and mortality worldwide for 36 cancers in 185 countries," *CA. Cancer J. Clin.*, vol. 68, no. 6, pp. 394–424, Nov. 2018, doi: 10.3322/caac.21492.
- [3] "Cancer Today," *Cancer Today*, 1984. https://gco.iarc.fr/today/online-analysis-multi-bars?v=2020&mode=cancer&mode_population=countries&population=900&populations=905_840&key=asr&sex=0&cancer=39&type=0&statistic=5&prevalence=0&population_group=0&ages_group%5B%5D=0&ages_group%5B%5D=17&nb_items (accessed Jan. 15, 2021).
- [4] "Key Statistics for Pancreatic Cancer," *American Cancer Society*, 2021. <https://www.cancer.org/cancer/pancreatic-cancer/about/key-statistics.html>.
- [5] A. Rosenzweig, "Increase in Pancreatic Cancer Diagnoses Expected in 2019 – Pancreatic Cancer Action Network," *Pancreatic Cancer Action Network*, Jan. 08, 2019. <https://www.pancan.org/news/increase-in-pancreatic-cancer-diagnoses-expected-in-2019/> (accessed Jan. 15, 2021).
- [6] Y. Yang, "THE THROMBOSIS PATHWAY PROMOTES PANCREATIC CANCER GROWTH AND METASTASIS," Purdue University Graduate School, 2019.
- [7] P. Metharom, M. Falasca, and M. C. Berndt, "The History of Armand Trousseau and Cancer-Associated Thrombosis," *Cancers (Basel)*, doi: 10.3390/cancers11020158.
- [8] N. Binti, A. Razak, G. Jones, M. Bhandari, M. C. Berndt, and P. Metharom, "Cancer-Associated Thrombosis: An Overview of Mechanisms, Risk Factors, and Treatment," *Cancers (Basel)*, 2018, doi: 10.3390/cancers10100380.
- [9] A. A. Khorana, "Venous Thromboembolism and Prognosis in Cancer," *Thromb Res*, vol. 125, no. 6, pp. 490–493, 2010, doi: 10.1016/j.thromres.2009.12.023.
- [10] A. A. Khorana and G. C. Connolly, "Assessing Risk of Venous Thromboembolism in the Patient With Cancer," *J Clin Oncol*, vol. 27, pp. 4839–4847, 2009, doi: 10.1200/JCO.2009.22.3271.
- [11] A. A. Khorana and R. L. Fine, "Pancreatic cancer and thromboembolic disease," *Lancet Oncol.*, vol. 5, no. 11, pp. 655–663, Nov. 2004, doi: 10.1016/S1470-2045(04)01606-7.
- [12] S. P. Grover and N. Mackman, "Tissue Factor: An Essential Mediator of Hemostasis and Trigger of Thrombosis," *Arterioscler. Thromb. Vasc. Biol.*, vol. 38, no. 4, pp. 709–725, Apr. 2018, doi: 10.1161/ATVBAHA.117.309846.
- [13] Y. Hisada and N. Mackman, "Tissue Factor and Cancer: Regulation, Tumor Growth and Metastasis," doi: 10.1055/s-0039-1687894.
- [14] J. W. Weisel and R. I. Litvinov, "Fibrin Formation, Structure and Properties," *Subcell. Biochem.*, vol. 82, pp. 405–456, 2017, doi: 10.1007/978-3-319-49674-0_13.
- [15] T. S. Nguyen, T. Lapidot, and W. Ruf, "Extravascular coagulation in hematopoietic stem and progenitor cell regulation," vol. 132, no. 2, pp. 123–131, 2018, doi: 10.1182/blood-2017-12-768986.

- [16] D. R. Senger, C. A. Perruzzi, A. Papadopoulos-Sergiou, and L. Van De Water, “Adhesive properties of osteopontin: Regulation by a naturally occurring thrombin-cleavage in close proximity to the GRGDS cell-binding domain,” *Mol. Biol. Cell*, vol. 5, no. 5, pp. 565–574, 1994, doi: 10.1091/mbc.5.5.565.
- [17] D. M. Heuberger and R. A. Schuepbach, “Protease-activated receptors (PARs): Mechanisms of action and potential therapeutic modulators in PAR-driven inflammatory diseases,” *Thrombosis Journal*, vol. 17, no. 1. BioMed Central Ltd., p. 4, Mar. 29, 2019, doi: 10.1186/s12959-019-0194-8.
- [18] M. Z. Wojtukiewicz, D. Hempel, E. Sierko, S. C. Tucker, and K. V Honn, “Thrombin—unique coagulation system protein with multifaceted impacts on cancer and metastasis,” *Cancer Metastasis Rev.*, vol. 35, no. 2, pp. 213–233, Jun. 2016, doi: 10.1007/s10555-016-9626-0.
- [19] J. Zain, Y. Q. Huang, X. S. Feng, M. L. Nierodzik, J. J. Li, and S. Karparkin, “Concentration-dependent dual effect of thrombin on impaired growth/apoptosis or mitogenesis in tumor cells,” *Blood*, vol. 95, no. 10, pp. 3133–3138, 2000, doi: 10.1182/blood.v95.10.3133.010k31_3133_3138.
- [20] D. Darmoul, V. Rie Gratio, H. Lè Ne Devaud, F. Peiretti, and M. Laburthe, “Activation of Proteinase-Activated Receptor 1 Promotes Human Colon Cancer Cell Proliferation Through Epidermal Growth Factor Receptor Transactivation,” 2004.
- [21] Y. Yang *et al.*, “Thrombin signaling promotes pancreatic adenocarcinoma through PAR-1—dependent immune evasion,” *Cancer Res.*, vol. 79, no. 13, pp. 3417–3430, Jul. 2019, doi: 10.1158/0008-5472.CAN-18-3206.
- [22] C. Tekin, K. Shi, J. B. Daalhuisen, M. S. T. Brink, M. F. Bijlsma, and C. A. Spek, “PAR1 signaling on tumor cells limits tumor growth by maintaining a mesenchymal phenotype in pancreatic cancer,” *Oncotarget*, vol. 9, no. 62, pp. 32010–32023, Aug. 2018, doi: 10.18632/oncotarget.25880.
- [23] K. C. S. Queiroz *et al.*, “Protease-activated receptor-1 drives pancreatic cancer progression and chemoresistance,” *Int. J. Cancer*, vol. 135, no. 10, pp. 2294–2304, Nov. 2014, doi: 10.1002/ijc.28726.
- [24] G. N. Adams *et al.*, “Colon cancer growth and dissemination relies upon thrombin, Stromal PAR-1, and fibrinogen,” *Cancer Res.*, vol. 75, no. 19, pp. 4235–4243, Oct. 2015, doi: 10.1158/0008-5472.CAN-15-0964.
- [25] A. J. Rice *et al.*, “Matrix stiffness induces epithelial–mesenchymal transition and promotes chemoresistance in pancreatic cancer cells,” *Oncogenesis*, vol. 6, no. 7, p. e352, Jul. 2017, doi: 10.1038/oncsis.2017.54.
- [26] E. Tomás-Bort, M. Kieler, S. Sharma, J. B. Candido, and D. Loessner, “3D approaches to model the tumor microenvironment of pancreatic cancer,” *Theranostics*, vol. 10, no. 11. Ivyspring International Publisher, pp. 5074–5089, 2020, doi: 10.7150/thno.42441.
- [27] D. Thomas and P. Radhakrishnan, “Tumor-stromal crosstalk in pancreatic cancer and tissue fibrosis,” *Mol. Cancer*, vol. 18, no. 1, p. 14, Dec. 2019, doi: 10.1186/s12943-018-0927-5.
- [28] Y. Liu *et al.*, “Fibrin stiffness mediates dormancy of tumor-repopulating cells via a Cdc42-driven Tet2 epigenetic program,” *Cancer Res.*, vol. 78, no. 14, pp. 3926–3937, Jul. 2018, doi: 10.1158/0008-5472.CAN-17-3719.
- [29] R. T. Kendall and C. A. Feghali-Bostwick, “Fibroblasts in fibrosis: novel roles and mediators,” *Front. Pharmacol.*, vol. 5, 2014, doi: 10.3389/fphar.2014.00123.

- [30] B. A. Pereira *et al.*, “CAF Subpopulations: A New Reservoir of Stromal Targets in Pancreatic Cancer,” *Trends in Cancer*, vol. 5, no. 11. Cell Press, pp. 724–741, Nov. 01, 2019, doi: 10.1016/j.trecan.2019.09.010.
- [31] W. M. Hall and P. Ganguly, “DIFFERENTIAL EFFECT OF THROMBIN ON THE GROWTH OF HUMAN FIBROBLASTS.”
- [32] A. N. Snead and P. A. Insel, “Defining the cellular repertoire of GPCRs identifies a profibrotic role for the most highly expressed receptor, protease-activated receptor 1, in cardiac fibroblasts,” *FASEB J.*, vol. 26, no. 11, pp. 4540–4547, Nov. 2012, doi: 10.1096/fj.12-213496.
- [33] J. Pohl, H. D. Bruhn, and E. Christophers, “Thrombin and fibrin-induced growth of fibroblasts: Role in wound repair and thrombus organization,” *Klin. Wochenschr.*, vol. 57, no. 6, pp. 273–277, Mar. 1979, doi: 10.1007/BF01476508.
- [34] M. R. D’andrea, C. K. Derian, R. J. Santulli, and P. Andrade-Gordon, “Differential Expression of Protease-Activated Receptors-1 and -2 in Stromal Fibroblasts of Normal, Benign, and Malignant Human Tissues,” 2001. doi: 10.1016/S0002-9440(10)64675-5.
- [35] J. Varennes, H. Moon, S. Saha, A. Mugler, and B. Han, “Physical constraints on accuracy and persistence during breast cancer cell chemotaxis,” *PLOS Comput. Biol.*, vol. 15, no. 4, p. e1006961, Apr. 2019, doi: 10.1371/journal.pcbi.1006961.
- [36] H. R. Moon, A. Ozcelikkale, Y. Yang, B. D. Elzey, S. F. Konieczny, and B. Han, “An engineered pancreatic cancer model with intra-tumoral heterogeneity of driver mutations,” *Lab Chip*, vol. 20, no. 20, pp. 3720–3732, Oct. 2020, doi: 10.1039/d0lc00707b.
- [37] A. Ozcelikkale *et al.*, “Differential response to doxorubicin in breast cancer subtypes simulated by a microfluidic tumor model,” *J. Control. Release*, vol. 266, pp. 129–139, Nov. 2017, doi: 10.1016/j.jconrel.2017.09.024.
- [38] T. Kolenda *et al.*, “State of the art paper 2D and 3D cell cultures-a comparison of different types of cancer cell cultures,” 2016, doi: 10.5114/aoms.2016.63743.
- [39] X. Liu, J. Yu, S. Song, X. Yue, and Q. Li, “Protease-activated receptor-1 (PAR-1): A promising molecular target for cancer,” *Oncotarget*, vol. 8, no. 63, pp. 107334–107345, 2017, doi: 10.18632/oncotarget.21015.
- [40] Kun-hwaHsieh, “THROMBIN INTERACTION WITH FIBRIN POLYMERIZATION SITES,” 1997.
- [41] P. G. Schweickert *et al.*, “Thrombin-PAR1 signaling in pancreatic cancer promotes an immunosuppressive microenvironment,” *J. Thromb. Haemost.*, vol. 19, no. 1, pp. 161–172, Jan. 2021, doi: 10.1111/jth.15115.
- [42] C. Qu, Q. Wang, Z. Meng, and P. Wang, “Cancer-Associated Fibroblasts in Pancreatic Cancer: Should They Be Deleted or Reeducated?,” *Integrative Cancer Therapies*, vol. 17, no. 4. SAGE Publications Inc., pp. 1016–1019, Dec. 01, 2018, doi: 10.1177/1534735418794884.
- [43] J. P. Biggerstaff, B. Weidow, J. Vidosh, J. Dexheimer, S. Patel, and P. Patel, “Soluble fibrin inhibits monocyte adherence and cytotoxicity against tumor cells: Implications for cancer metastasis,” *Thromb. J.*, vol. 4, no. 1, p. 12, Aug. 2006, doi: 10.1186/1477-9560-4-12.

APPENDIX

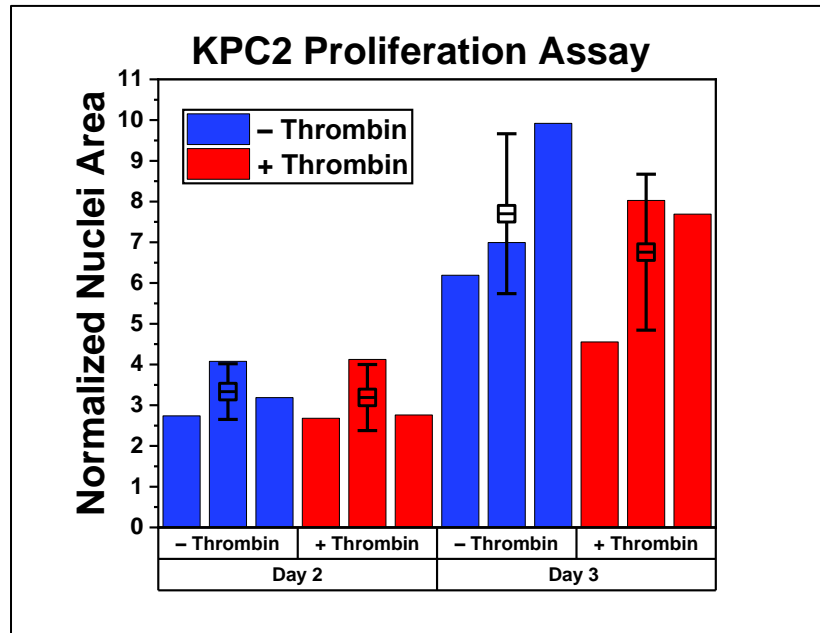


Figure 12: Results from KPC2 proliferation assay. Note: The boxed horizontal bar indicates the mean, while the error bars are the standard deviation for that dataset.

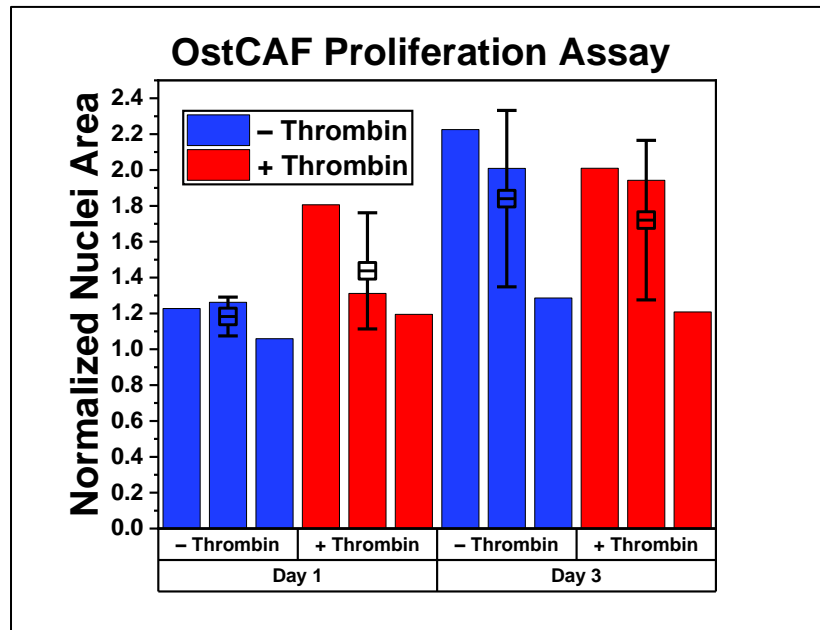


Figure 13: Results from OstCAF proliferation assay. Note: The boxed horizontal bar indicates the mean, while the error bars are the standard deviation for that dataset.

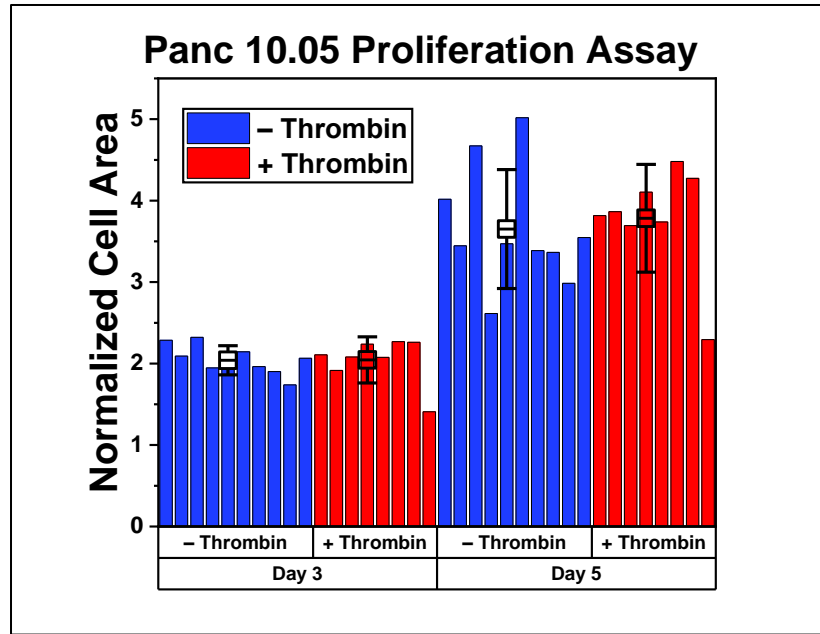


Figure 14: Results from Panc 10.05 proliferation assay. Note: The boxed horizontal bar indicates the mean, while the error bars are the standard deviation for that dataset.

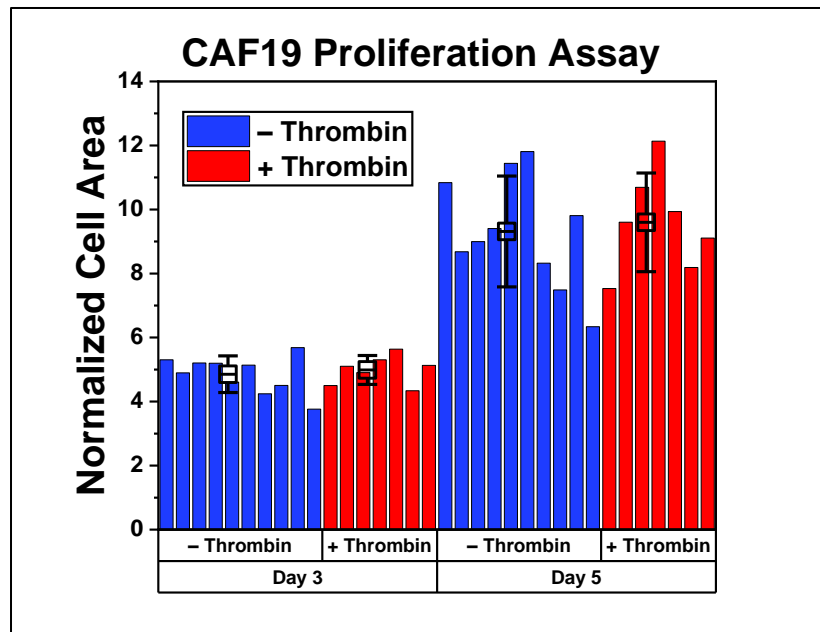


Figure 15: Results from CAF19 proliferation assay. Note: The boxed horizontal bar indicates the mean, while the error bars are the standard deviation for that dataset.

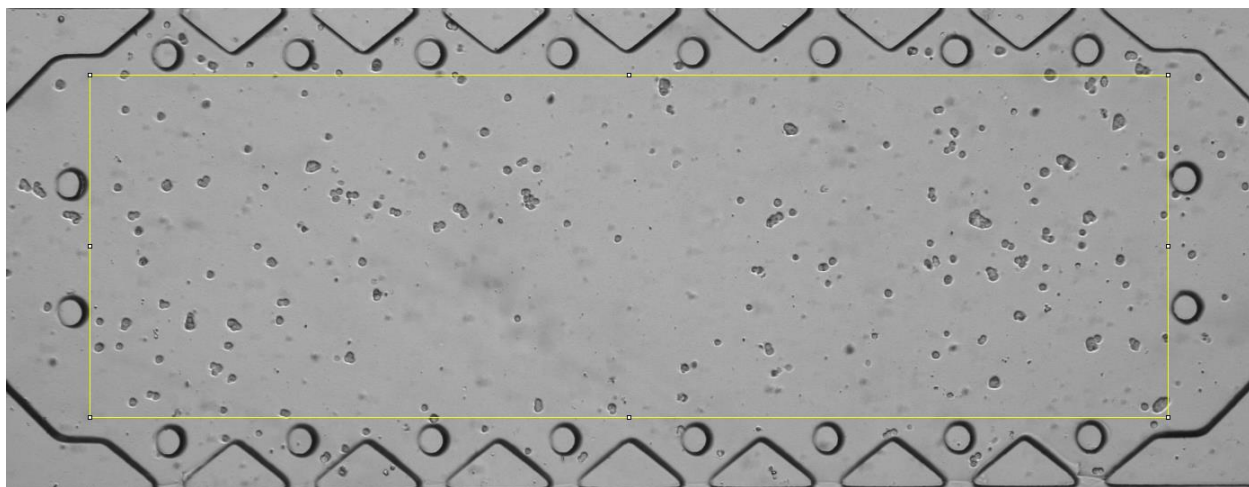


Figure 16: ROI for quantifying cell proliferation.